A | R | J
Amrit Research Journal December 2022, Vol. 3, Issue 1, 101-108
ISSN: 2738-9553
RESEARCH ARTICLE

Effect of Permittivity of Plasma Medium on the Particle Properties and Electric Field in a Magnetized Plasma Sheath

Prem Dahal[1] , Roshan Chalise[1, 2*], Raju Khanal[2]
[1]Amrit Campus, Tribhuvan University, Lainchaur, Kathmandu, Nepal
[2]Central Department of Physics, Tribhuvan University, Kirtipur, Kathmandu, Nepal
Email: plasma.roshan@gmail.com

(Received: August 18, 2022, Received in revised form: November 15, Accepted: December 2, 2022, Available Online)

Highlights

- Ion and electron densities, potential, electric field and space charge density in magnetized plasma sheath for various permittivity of plasma medium are studied using the Kinetic trajectory simulation method.
- The plasma parameters in magnetized plasma sheath regime may be controlled by controlling the permittivity in plasma medium.
- The results are qualitatively more accurate and provide a better understanding of the plasma-wall transition phenomena.

Abstract

The plasma sheath, a thin layer having sharp gradients, is necessary to be formed at any material wall in exposure with plasma for its stability. Characteristics of magnetized plasma sheath formed in front of a material wall for different permittivity of plasma medium has been studies using the kinetic trajectory simulation (KTS) model. The electron density, ion density, electric field and potential decreases on moving away from the sheath entrance but total charge density increases. As plasma is composed of charged particles, any variation in the permittivity of the medium has significant effects on the sheath properties. It is found that on increasing the permittivity of the medium, the electric potential strength and hence electric field decreases because of increased shielding ability of the plasma. The results are in qualitative agreement with earlier studies based on the fluid approach but the kinetic approach is more accurate quantitatively providing a better perception of plasma-wall transition phenomena.

Keywords: *Bohm criterion, Bohm-Chodura condition, kinetic trajectory simulation, plasma-wall interaction, magnetized plasma sheath*

Introduction

The behavior of plasma at material wall of a container is always a fascinating event which is one of the olderst problems in plasma [1] and is still not fully understood [2-7]. A thin layer that is formed close to a wall facing plasma and has sharp gradients is known as the plasma sheath. I. Langmuir disclosed the basic characters of plasma-sheath transition region [1]. D. Bohm studied interaction of positive ion space charges and electron in sheaths and the nature of the Bohm criterion was used in an indirect form [8]. R. Chodura [9] deliberated the consequence of an oblique magnetic field on the plasma-wall region using numerical model to calculate the motion of plasma particles and generalized Bohm criterion. The transition region has a two structure; a quasineutral magnetic presheath region followed by an electrostatic Debye sheath. K U. Riemann [10] found that the region near the negative absorbing wall split into collisionless planner space-charge sheath and quasi-neutral presheath, where ions are accelerated up to the ion-acoustic velocity by the electric field penetrating the plasma. R. Chalise and R. Khanal [11] used the KTS for magnetized plasma sheath and found that the magnetic effect is strong near the sheath entrance. KTS model was further

[*]Corresponding author

modified and extended in studying different magnetized plasma sheath problems [3, 12-15]. S. Farhad and M. Khoramabadi [16] studied the properties of the collisional magnetized sheath with two species of positive ions by using the fluid model. Their analysis demonstrated that sheath dynamic is responsive to the power-law dependency, mainly for ions with higher density. G. C. Chen *et al.* [17] used N_2, O_2, and N_2-O_2 mixture as the working medium gas of a plasma igniter to study the influence of the gas medium. The emission spectra of the plasma jet had markedly differences when different working gases were used in the igniter. S. Basnet, A. Sarma, and R. Khanal [15] studied plasma-wall interaction at diverse electron temperatures and found that effect of temperature is dominant in the sheath. They found that the increase in temperature also increases the magnitude of potential and field due to this their respective densities are varied. In this work, we have studied the effect in permittivity of plasma medium on particle properties (profiles of ion density, electron density, total charge density) and electric field in magnetized plasma sheath by employing the KTS method, suitable for studying the magnetized plasma-wall transition region.

Model

As the plasma particles are directed from the sheath entrance towards the boundary by strong electric field, we consider *1d3v* model for the sheath region [12] is as shown in figure. 1. Here electric field is acts along the *x*-axis so we consider the plasma parameter to vary only along the *x*-direction. The right-hand boundary is the sheath entrance which divides collisionless and non-neutral sheath regime from the bulk plasma and the left-hand boundary is the material wall.

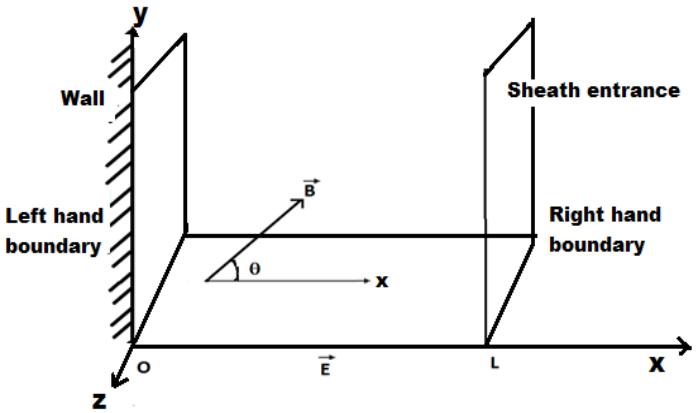

Fig 1. 1d3v model of plasma sheath region [12].

The angle constructed by the magnetic field along normal to the wall is denoted by θ:

$$\vec{B} = B_0[cos\theta\dot{x} + sin\theta\dot{y}] \quad (1)$$

The plasma particles enter the simulation region from the right-hand boundary with cut-off Maxwellian velocity distributions; the left-hand boundary absorbs some fraction of particles that depends on the energy of incident particles. Due to this, the distribution functions of electrons will become

$$f^e(x,v) = A^e \exp\left[-\left(\frac{v_x^2 + v_y^2 + v_z^2}{v^{e2}}\right) + \frac{e\phi(x)}{kT^e}\right]\Theta\left[v_c^e(x) - v_x\right] \quad (2)$$

where, $v_c^e(x) = \sqrt{\frac{2e[\phi(x) - \phi_0]}{m^e}}$, is the electron cut-off velocity at *x*. Ion velocity distribution function at right hand boundary is given by $f^i(L,v) = A^i \exp\left[-\left(\frac{(v_x - v_{mL}^i)^2 + v_y^2 + v_z^2}{v^{i2}}\right)\right] \Theta\left(v_{cL}^i - v_x\right)$ (3)

where A^i, T^i, v^i_{mL}, v^i_{cL},, T^e, v^e_{cL} are considered according to the specified conditions $\Theta(x)$ is the Heaviside step function.

Kinetic Trajectory Simulation (KTS) Method

In KTS method, velocity distribution functions of particle species involved are directly calculated by solving the related kinetic equations along the respective collisionless particle trajectories [18]. To calculate the distribution function at any point of the phase-space we trace the respective trajectories of phase-space where the distribution function is known. We assumed that electron and ion velocity distribution functions at the sheath edge to be cut-off Maxwellian. For species-*s* velocity distribution function satisfies the kinetic equation

$$\frac{df^s}{dt} = \left(\frac{\partial}{\partial t} + \vec{v}.\frac{\partial}{\partial \vec{x}} + \overrightarrow{a^s}.\frac{\partial}{\partial \vec{v}}\right) f^s(\vec{x},\vec{v}) = C_s \quad (4)$$

where, $\overrightarrow{a^s}(\vec{x},\vec{v},t) = \frac{q^s}{m^s}\left[\vec{E}(\vec{x},t) + \vec{v} \times \vec{B}(\vec{x},\vec{t})\right]$ *s = (e, i)*

Here, locally averaged electric and magnetic fields are $\vec{E}(\vec{x},t)$, $\vec{B}(\vec{x},t)$ and the macroscopic acceleration of the species-*s* particles is $\overrightarrow{a^s}(\vec{x},\vec{v},t)$, and C_s is the species-*s* collision term. In collisionless cases, the kinetic equation takes the familiar form of the Vlasov equation:

$$\left(\frac{\partial}{\partial t} + \vec{v}.\frac{\partial}{\partial \vec{x}} + \overrightarrow{a^s}.\frac{\partial}{\partial \vec{v}}\right) f^s(\vec{x},\vec{v}) = 0 \quad (5)$$

i.e, $\frac{df^s}{dt} = 0$, which gives $f^s(\mathrm{x},\mathrm{v}) = \mathrm{constant}$.

Once the distribution functions are calculated, then electron and ion densities are calculated using

$$n^s = \int_{-\infty}^{+\infty} f^s(x,v)dv \quad (6)$$

and the space charge density is

$$\rho(x) = \sum q^s\, n^s \quad (7)$$

The electrostatic potential $\varphi(x)$ is obtained by solving the Poisson's equation

$$\frac{\mathrm{d}^2\varphi(\mathrm{x})}{\mathrm{dx}^2} = \frac{-\rho(x)}{\varepsilon_0\epsilon_r} \quad (8)$$

then the electric field is calculated using

$$E = -\nabla(\varphi) \quad (9)$$

Results and Discussion

The different profiles of plasma parameters in the sheath region are obtained for plasma medium having different dielectric constants at fixed magnitude (0.5 mT) and obliqueness (θ = 30°) of the magnetic field. The ion density profile in the sheath region for three different values of the permittivity of the plasma medium is shown in Fig. 2. In this, and subsequent figures, the distance is measured from the wall and is normalized by the electron Debye length at the sheath entrance. The ion density goes on decreasing as we move away from the sheath entrance towards the wall which clearly shows that the variation of ion density is more near the boundaries. Also, the decrement in ion density is more with an increase in dielectric constant of plasma medium. For different permittivity of plasma medium nature of ion density profile is similar; however, the increased dielectric nature is more effective in screening the potential thereby causing a decrease in ion density reaching the wall.

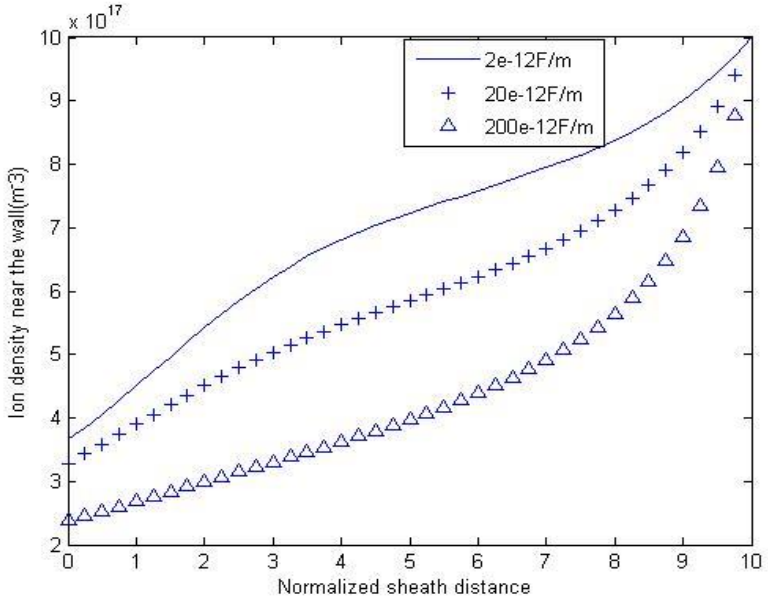

Fig 2. Ions density versus normalized distance for three different permittivity.

Ion density variation at the wall for different permittivity of the plasma medium for all other parameters being the same is showed in Fig. 3. The ion density at wall is appropriately best fitted as an exponential function $y = 2.96 \text{ x } 10^{17} e^{(-1310654767.17x)}$ which is continuously decreasing in the given range of permittivity. The reason for such a profile of ion density at wall is attributed to the fact that strength of potential goes on decreasing with permittivity. This will cause only the energetic ions to reach the wall.

The variation of electron density versus normalized sheath distance for diverse values of permittivity of plasma medium are shown in Fig. 4. Nature of the profile is almost similar as that of ions but the decrement is faster in moving towards the wall from the sheath entrance.

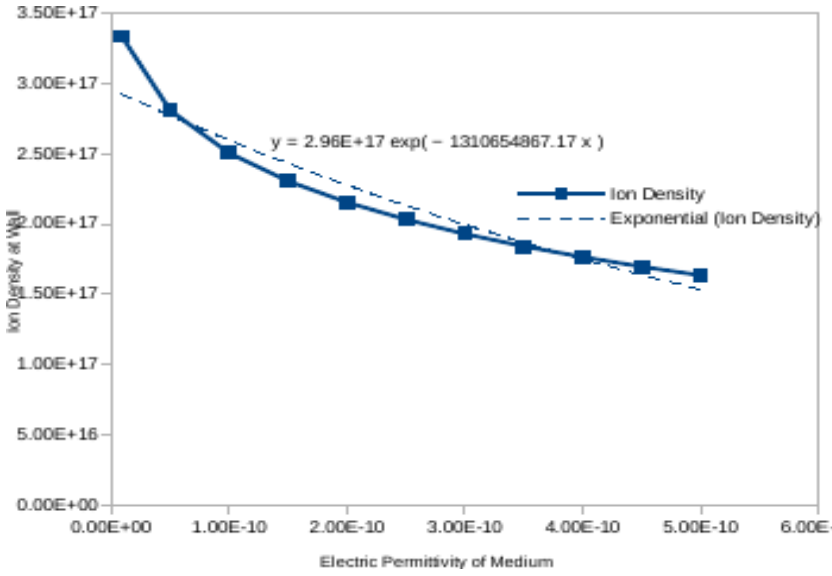

Fig 3. Variation of ions density at the wall for different permittivity of the plasma medium.

The number density decreases with an increase in dielectric constant value of plasma medium. Since wall is at a negative potential, electrons are strongly rejected from it due to the Coulomb repulsion and the wall receives only electrons having high thermal velocity.

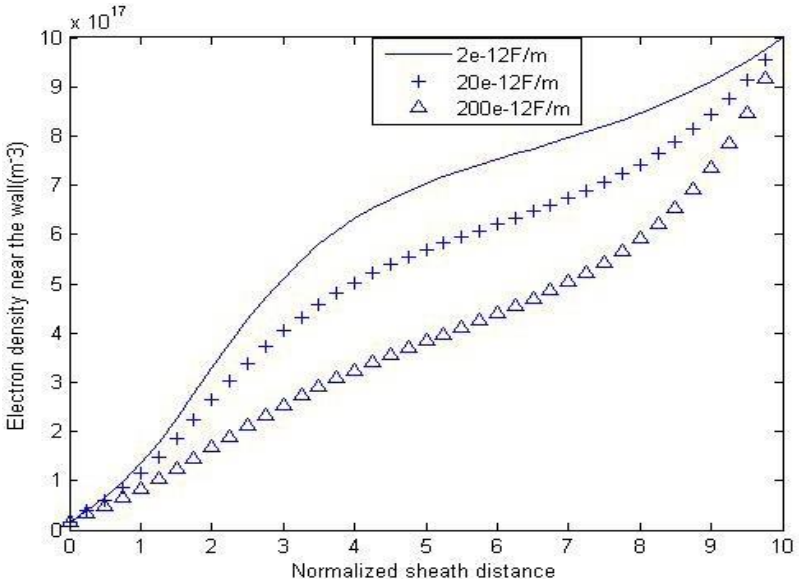

Fig 4. Electrons density versus with normalized distance for different permittivity of plasma medium.

Fig. 5 illustrates the variation of total charge density changes with normalized sheath distance for different values of the permittivity of the plasma medium. It shows that the total charge density increases towards wall and increment near the wall and sheath boundary is sharper which becomes almost flat in the middle. On increasing the dielectric constant of the medium in the plasma system decrement in the total charge density is observed which is dominant on either boundary. Variation of total charge density at wall with variation of the permittivity in plasma medium is shown in Fig. 6. The functional profile of total charge density at wall is well estimated by best fitting at exponential curve $y = 0.05e^{(14140714859.2x)}$ which is continuously decreasing in the given range of permittivity.

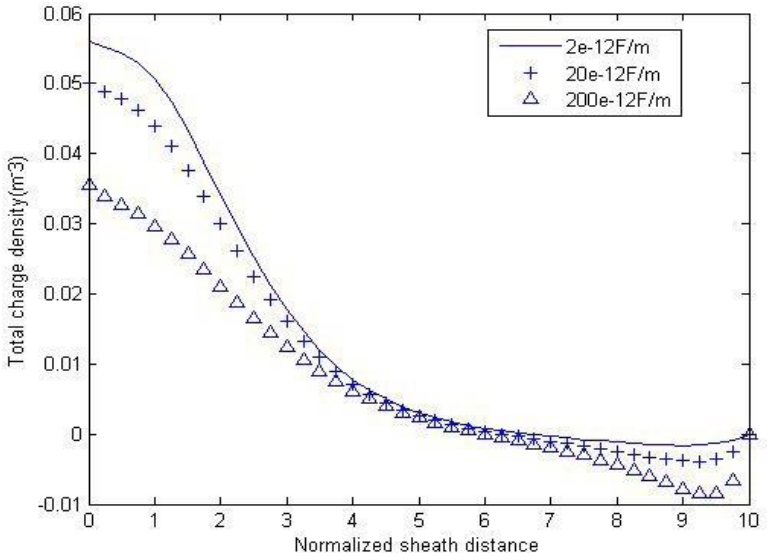

Fig 5. Total charge density versus with normalized distances for different permittivity of the plasma medium.

The variation of potential versus normalized sheath distance for different values of permittivity of the plasma medium is shown in Fig. 7. Potential declines in moving towards wall but potential variation in central sheath region is more flat compared to the region near the wall. The increment of electric permittivity of the medium decreases the potential and the effect of variation of electric permittivity becomes more dominant in the central region.

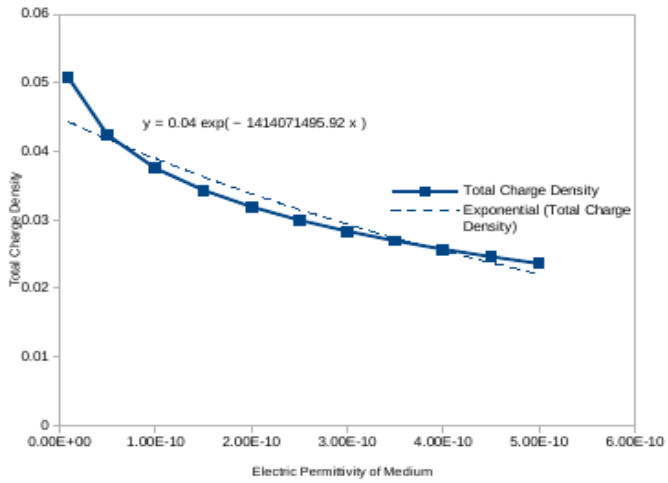

Fig 6. Total charge density at the wall for diverse value of permittivity of the plasma medium

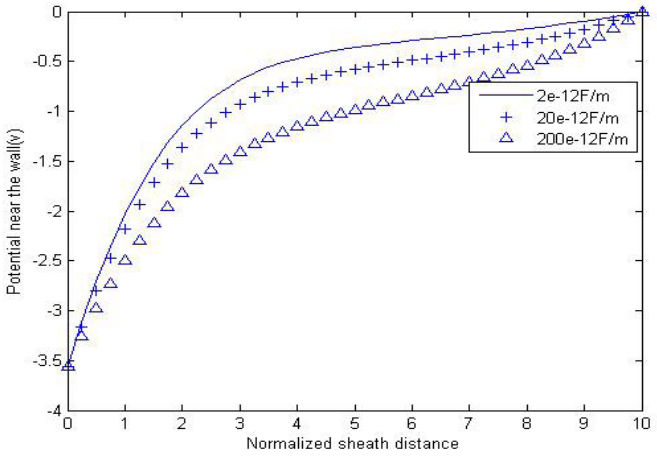

Fig. 7. Potential versus normalized distance for three different permittivity of the plasma medium.

The variation of electric field versus normalized sheath distance for different plasma mediums are shown in Fig. 8. The field becomes more negative in moving towards the wall and the increment of permittivity of the plasma medium further enhances the electric field. The profile of the electric field strength at the wall for different permittivity of the plasma medium is shown in Fig. 9. The functional profile of the electric field at the wall is well predicted by the best fitted exponential curve $y = -72728e^{(-42630247264.4x)}$ which is continuously increasing in the given range of permittivity.

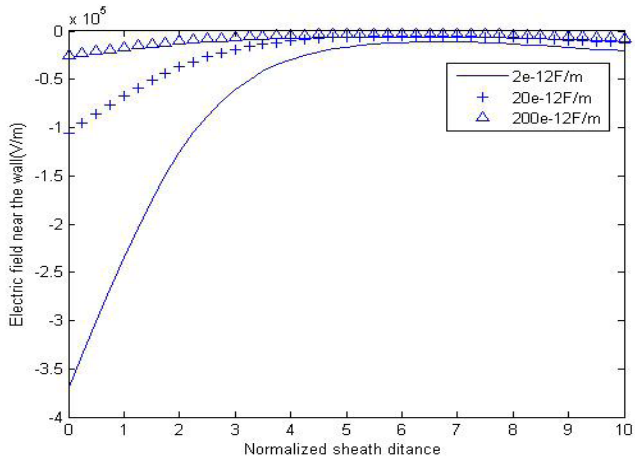

Fig 8. Electric field against normalized distance for different permittivity of the plasma medium.

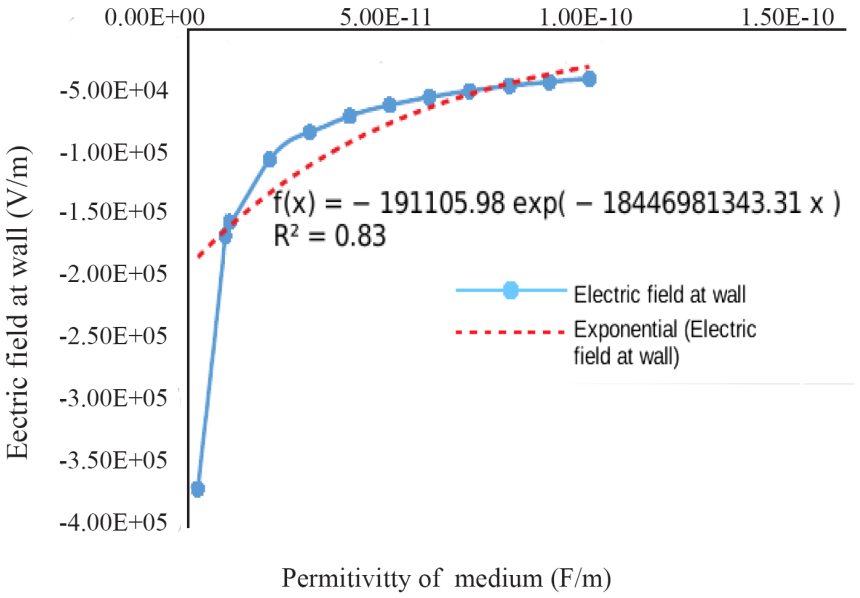

Fig 9. Variation of electric field at wall for different permittivity of the plasma medium.

Conclusions

The effect of the permittivity of the medium in a plasma system comprising charged particles causes variations in their strength of electric field and potential. It is clear that on increasing the permittivity of the medium the strength of potential and field decreases. The electron density, ion density, electric field and potential goes on decreasing in moving towards materials wall from the sheath entrance but total charge increases. With an increase in the permittivity of the medium, the variations become even more distinct. The results are comparable with previous works; based on fluid model [16] and experimental results [17]; showing qualitative similarity. As the kinetic approach gives the most reliable results compared to the fluid model our results are expected to provide a better understanding of the plasma-wall transition phenomena.

Acknowledgements

The corresponding author (Roshan Chalise) would like to acknowledge University Grants Commission, Nepal for PhD fellowship award (PhD-78/79-S & T-16).

References

1. I. Langmuir, Oscillations in ionized gases, *Proceedings of the National Academy of Sciences of the United States of America*, (1928), *14*(8), 627. http://dx.doi.org/10.1073/pnas.14.8.627
2. L. Kos, N. Jelić, T. Gyergyek, S. Kuhn, and D. D. Tskhakaya, Modeling and simulations of plasma and sheath edges in warm-ion collision-free discharges, *AIP Advances,* (2018), *8*, 105311. https://doi.org/10.1063/1.5044664
3. S. Basnet and R. Khanal, Kinetic trajectory simulation method for the multi-component magnetized plasma sheath, *Plasma Physics and Controlled Fusion*, (2019), 61, 065022. https://doi.org/10.1088/1361-6587/ab1708
4. R. Sahu, A. R. Mansour, and K. Hara, Full fluid moment model for low temperature magnetized plasmas, *Physics of Plasmas*, (2020), 27, 113505. https://doi.org/10.1063/5.0021474
5. A. Alvarez-Laguna, T. Magin, M. Massot, A. Bourdon, and P. Chabert, Plasma-sheath transition in multi-fluid models with inertial terms under low-pressure conditions: comparison with the classical and kinetic theory, *Plasma Sources Science and Technology*, (2020), 29(2), 025003. https://doi.org/10.1088/1361-6595/ab6242

6. Chalise, R., Nepali, B., Thakur, G., Basnet, S., & Khanal, R. Effect of Negative Ion Concentration and Magnetic Field on Electronegative Plasma Sheath. *Tribhuvan University Journal*, (2021), *36*(02), 1-13. https://doi.org/10.3126/tuj.v36i02.46593
7. A. Deuja, S. Basnet, and R. Khanal, Effect of non-uniform magnetic field on two ion species plasma-wall transition, *Plasma Physics and Controlled Fusion*, (2022), 64, 025004. https://doi.org/10.1088/1361-6587/ac3c3b
8. D. Bohm, *The Characteristic of Electrical Discharges in Magnetic Fields,* Edited by A. Guthry and R. K. Wakerling, McGraw-Hill, New York, (1949), 77.
9. R. Chodura, Plasma-wall transition in an oblique magnetic field, *Physics of Fluids,* (1982), 25, 1628. http://dx.doi.org/10.1063/1.863955
10. K. U. Riemann, The Bohm criterion and sheath formation, *Journal of Physics D: Applied Physics,* (1991), 24, 493. http://dx.doi.org/10.1088/0022-3727/24/4/001
11. R. Chalise and R. Khanal, A kinetic trajectory simulation model for magnetized plasma sheath, *Plasma Physics and Controlled Fusion*, (2012), 54, 095006. http://dx.doi.org/10.1088/0741-3335/54/9/095006
12. R. Chalise and R. Khanal, Self consistent one dimension in space and three dimension in velocity kinetic trajectory simulation model of magnetized plasma-wall transition, *Physics of Plasmas,* (2015), 22, 1135005. http://dx.doi.org/10.1063/1.4934601
13. Y. Regmi, R. Chalise and R. Khanal, Response of carbon and tungsten surfaces to hydrogen plasma of different temperatures, *Physics of Plasmas,* (2018), 25, 043521. https://doi.org/10.1063/1.5020386
14. R. Chalise, S. K. Pandit, G. Thakur and R. Khanal, Effect of electron temperature in a magnetized plasma sheath using kinetic trajectory simulation, *BIBECHANA,* (2020), 18, 58. https://doi.org/10.3126/bibechana.v18i1.29204
15. S. Basnet, A. Sarma and R. Khanal, Effect of presheath electron temperature on magnetized plasma-wall transition and wall sputtering by plasma having two species of positive ions. *Physica Scripta*, (2020), 95, 065601. https://doi.org/10.1088/1402-4896/ab7b89
16. S. Farhad and M. Khoramabadi, Magnetized plasma sheath with two positive ions where collision frequencies have a power law dependency on ions velocities, *Journal of Theoretical and Applied Physics*, (2015), 9, 307. https://doi.org/10.1007/s40094-015-0190-8
17. G. C Chen *et al.*, Effects of working medium gases on emission spectral and temperature characteristics of a plasma igniter, *Journal of Spectroscopy*, (2019), 2019, 5395914. https://doi.org/10.1155/2019/5395914
18. R. Khanal, *A kinetic trajectory simulation model for bounded plasmas*, PhD Thesis, Innsbruck University, Austria (2003).